



1 **High Yields of Formic Acid and Acetic Acid during Multi-generational
2 Oxidation of Toluene**

3 Hengqing Shen^{1,2}, Liubin Huang^{1*}, Yue Zhao³, Min Zhao¹, Yu Yang¹, Huan Li⁴, Huihui Wu²,
4 Zhongming Chen^{2*}

5 ¹Environment Research Institute, Shandong University, Qingdao, Shandong 266237, China

6 ²State Key Laboratory of Regional Environment and Sustainability, College of Environmental
7 Sciences and Engineering, Peking University, Beijing 100871, China

8 ³School of Environmental Science and Engineering, Shanghai Jiao Tong University, Shanghai
9 200240, China

10 ⁴China Center for Information Industry Development, Beijing 100871, China

11 ***Corresponding Author**

12 Liubin Huang (hliubin@sdu.edu.cn) and Zhongming Chen (zmchen@pku.edu.cn).



13 **ABSTRACT**

14 Formic acid and acetic acid are the most abundant gas-phase organic acids in the atmosphere,
15 yet their concentrations are substantially underestimated by both global and regional
16 atmospheric models across diverse environments. In this study, we report unexpectedly high
17 yields of formic acid and acetic acid formed during the multi-generational photooxidation of
18 toluene, a canonical anthropogenic volatile organic compound. Their yields show a strong
19 dependence on hydroxyl radical ($\cdot\text{OH}$) exposure ($[\cdot\text{OH}] \times$ residence time), increasing from 25%
20 and 24% under low exposure (<0.2 equivalent days) to 74% and 40% under elevated exposure
21 (1–3 equivalent days) for formic and acetic acid, respectively. The formation of these organic
22 acids is not significantly affected by NO_x concentrations. A modified box model based on MCM
23 v3.3.1 underestimates the peak concentrations of both acids by approximately a factor of five,
24 indicating substantial gaps in current mechanistic understanding. Although both secondary
25 aerosol formation and organic acid production increase with aging within a certain degree of
26 oxidation, their distinct temporal evolutions indicate that particle photodegradation is not the
27 dominant pathway. The contrasting $\cdot\text{OH}$ exposure dependence between organic acids and
28 primary carbonyl compounds further suggests that these acids are predominantly multi-
29 generational oxidation products. These findings demonstrate that multi-generational oxidation
30 of aromatic compounds is an important and previously underappreciated source of atmospheric
31 organic acids. The omission of organic acid formation from aromatic oxidation in current
32 chemical mechanisms likely contributes to their widespread underestimation in models,
33 highlighting the need for detailed laboratory studies and updated chemical mechanisms.

34



35 1 INTRODUCTION

36 Organic acids are ubiquitous in the troposphere and are important contributors to acidity in
37 precipitation (Stavrakou et al., 2012). Among them, formic acid (HCOOH) and acetic acid
38 (CH_3COOH) are the most abundant gas-phase organic acids in various atmospheric
39 environments, with mixing ratios spanning from a few parts per trillion by volume (pptv) to
40 tens of parts per billion by volume (ppbv) (Chebbi and Carlier, 1996; Veres et al., 2011; Mungall
41 et al., 2018; Ding et al., 2025). Formic acid alone can contribute to more than half of rainwater
42 acidity in many continental regions (Stavrakou et al., 2012). In addition, these organic acids can
43 also affect secondary aerosol formation by modifying aerosol pH and gas-particle partitioning
44 processes (Shen et al., 2018; Tao and Murphy, 2019).

45 On a global scale, the dominant source for formic acid and acetic acid is considered to be
46 secondary production from the photooxidation of biogenic volatile organic compounds (VOCs),
47 particularly isoprene and its oxidation products (Paulot et al., 2011; Khan et al., 2018; Link et
48 al., 2020). But rapid secondary production and high amounts of formic acid and acetic acid
49 have also been observed in anthropogenic air masses and urban environments (Veres et al., 2011;
50 Yuan et al., 2015; Millet et al., 2015; Liggio et al., 2017), suggesting that anthropogenic VOCs
51 may play a significant role in the formation of formic acid and acetic acid in the polluted areas.
52 However, sources of atmospheric organic acids and their detailed formation pathways are still
53 poorly understood, as evidenced by the fact that current atmospheric chemical models
54 substantially underestimate (up to >10 times) their field-observed concentrations on both global
55 (Paulot et al., 2011; Stavrakou et al., 2012; Chaliyakunnel et al., 2016; Khan et al., 2018) and
56 regional scales (Le Breton et al., 2012; Yuan et al., 2015; Millet et al., 2015; Liggio et al., 2017)
57 in the free troposphere (Paulot et al., 2011; Millet et al., 2015), the forest (Stavrakou et al., 2012;
58 Schobesberger et al., 2016), the urban (Yuan et al., 2015; Bannan et al., 2017; Khan et al., 2018),
59 the polar region (Paulot et al., 2011; Mungall et al., 2018), and the oil sands region (Yuan et al.,
60 2015; Liggio et al., 2017). Such widespread underestimation implies the existence of large and
61 pervasive missing or underestimated sources in current models (Yuan et al., 2015; Liggio et al.,
62 2017). Numerous hypotheses have been proposed to reconcile this model–observation gap,
63 including previously unrecognized contributions from biomass burning (Paulot et al., 2011;
64 Chaliyakunnel et al., 2016), unmeasured anthropogenic intermediate VOCs (Le Breton et al.,
65 2012; Liggio et al., 2017), acetaldehyde tautomerization (Shaw et al., 2018), cloud-mediated
66 methanediol oxidation (Franco et al., 2021), and chemical aging of organic aerosols (Paulot et
67 al., 2011; Malecha and Nizkorodov, 2016, 2017; Bates et al., 2023; Jiang et al., 2023).



68 Nevertheless, none of these processes alone can fully account for the high ambient
69 concentrations of formic acid and acetic acid observed in the atmosphere (Yuan et al., 2015;
70 Liggio et al., 2017; Franco et al., 2021).

71 Recent studies have suggested that resolving this discrepancy would require much higher
72 effective molar yields of formic acid from the oxidation of monoterpenes or anthropogenic
73 VOCs than currently assumed (Stavrakou et al., 2012; Liggio et al., 2017). For example, Liggio
74 et al. (2017) estimated that ~50% of formic acid yield would be necessary to reconcile
75 observations and modeling results in an oil sand region (Liggio et al., 2017). In contrast,
76 laboratory-reported yields of formic acid and acetic acid from VOC photooxidation are
77 typically below 15% (Berndt and Böge, 2001; Baltensperger et al., 2005; Paulot et al., 2011;
78 Yuan et al., 2015). Notably, most of these yields were measured under relatively low $\cdot\text{OH}$
79 exposures ($[\cdot\text{OH}] \times \text{residence time}$), corresponding to less than one equivalent atmospheric
80 photochemical day (Praplan et al., 2014). However, recent studies revealed that molecular
81 fragmentation reactions become increasingly important with oxidative aging (Lambe et al.,
82 2012; Ortega et al., 2013; Isaacman-VanWertz et al., 2018), potentially enhancing the formation
83 of small oxygenated species. Consistent with this hypothesis, substantial increases in gas-phase
84 organic acids have been observed during the aging of biomass-burning emissions (Ortega et al.,
85 2013; Bruns et al., 2017) and diesel exhaust (Friedman et al., 2017). For instance, Bruns et al.
86 (2017) reported that formic acid concentrations increased by factors of ~5–50 with aging.
87 Friedman and Farmer (2018) further demonstrated that the molar yield of organic acid strongly
88 depends on OH radical concentrations during photooxidation of monoterpenes. These findings
89 suggest that the persistent model–observation discrepancy may be owing to an incomplete
90 mechanistic and quantitative understanding of organic acid formation during multi-generational
91 oxidation under atmospherically relevant conditions.

92 Oxidation flow reactor (OFR) provides a powerful complement to traditional environmental
93 chambers by enabling simulation of oxidation equivalent to multiple days of atmospheric aging
94 within residence times of seconds to minutes through the use of elevated oxidant concentrations
95 (Lambe et al., 2015). A key advantage of OFR is its ability to achieve high photochemical
96 exposure while minimizing wall losses of gases and particles, which can be substantial in Teflon
97 chambers owing to the long residence times typically employed (Zhang et al., 2014; Brune,
98 2019). The validity of OFR has been demonstrated in numerous studies (Lambe et al., 2015;
99 Peng et al., 2015), and they are increasingly used to investigate the effects of photochemical
100 aging on gas-phase chemistry (Lambe et al., 2015; Friedman and Farmer, 2018), secondary

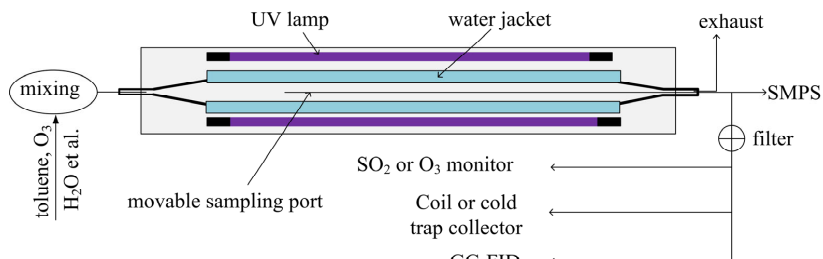


101 organic aerosol (SOA) formation (Bruns et al., 2015), and aerosol optical properties (Lambe et
102 al., 2013). In this study, we employ an OFR to investigate the formation of formic acid and
103 acetic acid during the photooxidation of toluene, a canonical and highly abundant
104 anthropogenic VOC, over a wide range of OH exposure, and examine how these processes
105 affected by relative humidity, initial toluene and NO_x concentration. By the combination of
106 laboratory studies and model simulations, the possible mechanism for the formation of formic
107 acid and acetic acid are also explored.

108 **2 METHODS**

109 **2.1 Oxidation Flow Reactor**

110 Toluene photooxidation experiments were conducted in a custom-built quartz oxidation flow
111 reactor (OFR) with a total volume of 2 L (1 m length and 5 cm inner diameter; Figure 1). The
112 reactor temperature was maintained at 298 K by a continuously circulating water jacket. Low-
113 pressure mercury lamps (primary emission at 254 nm) were evenly distributed around the
114 reactor, with up to eight lamps operating simultaneously. The OH radicals in the OFR were
115 generated via the reaction of O(¹D) + H₂O → 2 •OH, where O(¹D) was produced by photolysis
116 of externally introduced O₃. O₃ was generated upstream of the OFR using a custom-built O₃
117 generator in which O₂ was irradiated at 185 nm. Photons at 185 nm were effectively filtered by
118 the quartz sleeves of the lamps, the quartz reactor walls, and the water jacket, thereby
119 minimizing in situ O₃ formation inside the OFR (<10 ppbv). A movable sampling port (6 mm
120 outer diameter) enabled gas and particle sampling at different axial positions along the OFR.
121 The •OH exposure in the OFR was determined using the box model described in Section 2.3,
122 and the results are provided in Table S1 and Figure S1. At 20% RH, the modeled •OH exposures
123 ranged from 2.03×10^{10} to 1.97×10^{12} molecules cm⁻³ s, corresponding to equivalent
124 atmospheric aging of 0.07–6.34 days assuming a 24-h average OH radical concentration of 3.6×10^6 molecules cm⁻³ in urban Beijing (Tan et al., 2018). At 70% RH, the equivalent
125 atmospheric aging times in the experiments were from 0.20 to 15.64 days.
126



127

128 **Figure 1.** Schematic diagram of the experimental setup.



129 **2.2 Experimental Procedures**

130 Toluene gas with an initial concentration of ~94 ppbv was generated by passing a flow of N₂
131 (99.999%, Beijing Haipubeifen Gas) over liquid toluene (Merck, ≥ 99.9%) in a temperature-
132 controlled diffusion tube. RH in the OFR was adjusted by introducing water vapor generated
133 using a bubbler. The gas mixture of toluene, O₃, and water vapor were continuously introduced
134 into the OFR at a total flow rate of 2 L min⁻¹, and the initial concentration of O₃ was about 1580
135 ppbv. Samples were collected at axial positions corresponding to 5%, 25%, 45%, 65%, and 85%
136 of the reactor length using the movable sampling port. Under laminar flow conditions, these
137 positions corresponded to residence times of 3.9, 15.8, 27.5, 39.3, and 51.0 seconds,
138 respectively. Additional experiments were conducted with 2, 4, 6, or 8 lamps to achieve higher
139 •OH exposures. The corresponding •OH exposures under different experimental conditions are
140 summarized in Table S1. The influence of NO_x on organic acid formation was investigated by
141 adding N₂O to the OFR. NO and NO₂ were produced via the reaction O(¹D) + N₂O → 2 NO,
142 followed by NO + O₃ → NO₂ + O₂ (Lambe et al., 2017).

143 Toluene concentrations were quantified using gas chromatography with a flame ionization
144 detector (GC-FID, Agilent 7890A) (Wu et al., 2017). O₃ and SO₂ were measured using an O₃
145 analyzer (model 202, 2B Technologies, USA) and an SO₂ analyzer (model 43i-TLE, Thermo),
146 respectively. Particle number size distributions were measured using a scanning mobility
147 particle sizer (SMPS, DMA 3081 connected to CPC 3776, TSI Inc.). Carbonyl compounds were
148 collected using the cold trap method (Huang et al., 2013) and analyzed by high-performance
149 liquid chromatography (HPLC) with ultraviolet detection (Shen et al., 2018, 2024). All
150 experiments were conducted in the absence of seed particles. Gas-phase organic acids were
151 collected using a temperature-controlled scrubbing glass coil maintained at 277 K and extracted
152 with ultrapure water as the stripping solution (Wu et al., 2017; Xing et al., 2018). Gas and
153 stripping solution flow rates were 0.6 L min⁻¹ and 0.2 mL min⁻¹, respectively. The efficiency
154 of sample collection was measured as approximately 85% for acetic acid, 95% for formic acid,
155 and 99% for pyruvic acid. The eluent was collected for 15 min, and then the sample was
156 analyzed immediately using ion chromatography (DIONEX ICS-2000) (Shen et al., 2018). The
157 concentration of organic acids was quantified using a mixed liquid standard solution containing
158 formic acid, acetic acid, and pyruvic acid. To evaluate potential artifacts associated with
159 aqueous-phase formation in the stripping solution, five additional gas-phase samples were
160 collected using Horibe tubes with an ethanol cold trap maintained at 183 K. Concentrations
161 measured using the scrubbing coil and Horibe tubes agreed within 10%, indicating that



162 aqueous-phase artifacts had a minor influence on measurements. Reported yields of formic acid
163 and acetic acid in this study are apparent yields and were not corrected for their subsequent
164 reactions with OH radicals.

165 A series of control experiments was conducted to ensure data quality and reproducibility. (1)
166 Before each experiment, high concentrations of O₃ were introduced into the OFR with two
167 lamps illuminated until particle concentrations measured by the SMPS were negligible (< 50
168 cm⁻³) and no impurities were detected by GC-FID. (2) O₃ photolysis experiments were
169 performed before each toluene photooxidation experiment to verify consistent irradiation
170 conditions based on comparable O₃ decay rates. (3) Blank experiments were conducted without
171 toluene, with toluene but without O₃, and with both toluene and O₃ but without water vapor.
172 Formic and acetic acid concentrations observed in these blank experiments were low relative
173 to those measured during toluene photooxidation (less than 15%). All reported data were
174 corrected for blank contributions.

175 **2.3 Model Description and Determination of Photon Flux**

176 A zero-dimensional box model based on the Master Chemical Mechanism (MCM) v3.3.1
177 (<http://mcm.leeds.ac.uk/MCM/>) and modified following Li et al. (2015) was employed to
178 simulate toluene photooxidation and organic acid formation in the OFR (Li et al., 2015; Jenkin
179 et al., 2015). Rate coefficients for additional reactions were adopted from the latest JPL kinetic
180 evaluation (Li et al., 2015). Photolysis cross sections and quantum yields were taken from
181 Keller-Rudek et al. (2013) (Keller-Rudek et al., 2013). The initial concentrations of toluene, O₃,
182 and water vapor were set according to experimental conditions.

183 Accurate quantification of photon flux in the OFR is essential for determining photolysis rates
184 in the model. Direct measurement of photon flux is challenging due to attenuation by the water
185 jacket and quartz reactor walls. Therefore, photon flux in the OFR was determined by
186 combining model simulations with direct measurements of O₃ decay in experiments conducted
187 without toluene. The photon flux was iteratively adjusted in the model until the simulated O₃
188 decay rate matched the observed decay. Using this approach, the photon flux with one lamp
189 illuminated was estimated to be approximately 3.0×10^{15} photons cm⁻³ s⁻¹, consistent with
190 photon fluxes commonly used in OFR studies (Peng et al., 2016). Photon fluxes corresponding
191 to different numbers of illuminated lamps (up to eight) were determined using the same method,
192 and the results are shown in Figure S2. The validity of this approach for photon flux
193 determination, as well as the applicability of the box model to the OFR system, was further
194 evaluated by comparing simulated and measured SO₂ decay rates (Figure S3).



195 **3 RESULTS AND DISCUSSION**

196 **3.1 Production of Organic Acids in Toluene Photooxidation**

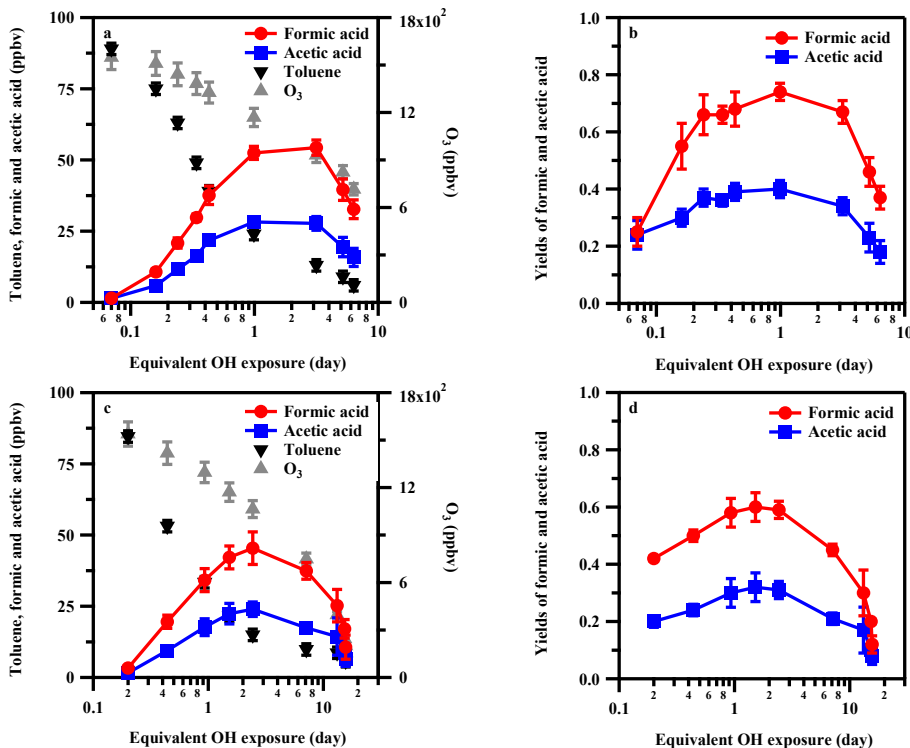
197 **3.1.1 •OH Exposure Dependence**

198 The major gas-phase organic acids observed during the photooxidation of toluene were formic
199 acid, acetic acid, and pyruvic acid, with minor contributions from lactic acid and oxalic acid
200 under both 20% and 70% RH conditions. Because formic acid and acetic acid together
201 accounted for approximately 90% of the total measured gas-phase organic acids, the following
202 analysis focuses primarily on these two species. Figure 2 illustrates the dependence of the
203 concentrations and molar yields of formic acid and acetic acid on •OH exposure. As •OH
204 exposure increased, their concentrations initially increased and subsequently decreased,
205 reaching maximum at approximately 1–3 equivalent days under both RH conditions. The
206 similar trends observed for formic acid and acetic acid suggest that their formation is governed
207 by closely related chemical pathways during toluene photooxidation. The decrease in organic
208 acid concentrations at higher •OH is primarily attributed to their continued reaction with OH
209 radicals after the complete consumption of toluene. At the highest •OH exposure investigated
210 (15.64 equivalent days), the concentrations of both acids decreased to about 25% of their
211 respective peak values. As shown in Figures 2a and 2c, the change of both formic acid and
212 acetic acid concentration with the increasing •OH exposure at 20% RH is similar to that at 70%
213 RH. However, it is found that organic acid concentrations were consistently higher under low
214 RH (20%) than under high RH (70%) at the identical OH exposures, suggesting that reactions
215 involving water vapor may play a limited role in organic acid formation in this study, in contrast
216 to the substantial contribution of stabilized Criegee intermediate–water reactions commonly
217 observed during alkene ozonolysis (Neeb et al., 1997; Orzechowska and Paulson, 2005; Kang
218 et al., 2025).

219 Figures 2b and 2d show a strong dependence of the molar yields of formic acid and acetic acid
220 (calculated relative to consumed toluene) on •OH exposure under both 20% and 70% RH
221 conditions. The yields increase from 25% (formic acid) and 24% (acetic acid) at low •OH
222 exposure (<0.2 equivalent days) to maximum values of 74% and 40%, respectively, at
223 intermediate •OH exposures (1–3 equivalent days). Previous studies have shown that molecular
224 fragmentation reactions become increasingly important under conditions of elevated •OH
225 exposure (Lambe et al., 2012; Ortega et al., 2013), which are difficult to achieve in traditional
226 environmental chamber experiments that typically span less than one equivalent day of
227 atmospheric aging. The pronounced increase in organic acid yields with •OH exposure suggests



228 that molecular fragmentation processes likely play an important role in formic acid and acetic
229 acid formation.



230 **Figure 2.** Production of formic acid and acetic acid during the photooxidation of toluene as a
231 function of •OH exposure. Panels (a) and (b) correspond to 20% RH, and panels (c) and (d)
232 correspond to 70% RH. The initial toluene concentration was ~94 ppbv. Error bars represent
233 standard deviations of repeated experiments under identical conditions.

234 Furthermore, we also compare the yields of formic acid and acetic acid measured from the
235 photooxidation of toluene with literature results. Seuwen and Warneck (1996) quantified the
236 yield of formic acid during the oxidation of toluene (Seuwen and Warneck, 1996), its yield
237 (approximately 13%) was more than five times lower than the peak value observed in our study.
238 In addition to toluene, the yields of formic and acetic acid produced from other aromatic
239 compounds reported by previous studies were also lower than our results (Gery et al., 1985;
240 Bandow and Washida, 1985; Bandow et al., 1985; Berndt et al., 1999; Wyche et al., 2009;
241 Müller et al., 2012). For example, Berndt et al. (1999) reported a formic acid yield of ~13%
242 from benzene oxidation, and Wyche et al. (2009) observed a formic acid yield of 14% from
243 1,3,5-trimethylbenzene under high-NO_x conditions (Berndt et al., 1999; Wyche et al., 2009).



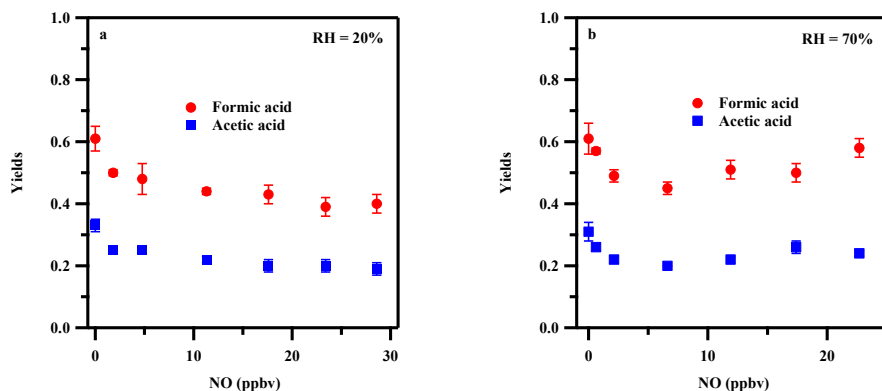
244 This discrepancy is likely due to differences in experimental conditions. Previous chamber
245 studies were typically conducted under relatively low •OH radical exposures, where primary
246 oxidation products dominate. In contrast, formic and acetic acids likely form as secondary or
247 later-generation products, which require higher •OH exposures (Lambe et al., 2012; Isaacman-
248 VanWertz et al., 2018; Drozd et al., 2019). Evidence supporting the role of higher •OH
249 exposures in organic acid formation comes from two previous studies. Wyche et al. (2009)
250 observed formic acid and acetic acid yields of 49% and 33%, respectively, during the
251 photooxidation of 1,3,5-trimethylbenzene under low-NO_x conditions, where the aromatic
252 precursor was nearly fully consumed (Wyche et al., 2009). Similarly, Murschell et al. (2018)
253 reported formic acid yields as high as 43% during the oxidation of the chlorinated aromatic
254 herbicide 2-methyl-4-chlorophenoxyacetic acid under very high •OH exposure (Murschell and
255 Farmer, 2018). Consistent with these findings, combustion studies, which effectively accelerate
256 atmospheric oxidation, also reported enhanced formation of formic and acetic acids from
257 toluene relative to non-aromatic compounds such as propane and isooctane (Zervas, 2005;
258 Battin-Leclerc et al., 2007). Additionally, previous experiments often used very high
259 concentrations of aromatic compounds (hundreds of ppb to ppm levels), which likely
260 suppressed •OH radical concentrations and limited effective oxidative aging. Our experiments
261 similarly show that increasing toluene concentrations inhibit the formation of organic acids. At
262 20% RH, the yield of formic acid decreased from 74% to 48% as the initial toluene
263 concentration increased from 94 to 381 ppbv. Together, these results highlight the critical role
264 of •OH exposure in controlling organic acid formation during aromatic oxidation. Further
265 discussion of these yield discrepancies is provided in Sections 3.2 and 3.3.

266 **3.1.2 NO_x Dependence**

267 Small organic acids, such as formic and acetic acid, are commonly thought to form via reactions
268 of peroxyacetyl radicals with HO₂/RO₂ radicals. The presence of NO_x is expected to suppress this
269 pathway by preferentially reacting with peroxy radicals, diverting them toward NO reaction
270 channels that favor nitrate and carbonyl formation over organic acid production. To investigate
271 the influence of NO_x on organic acid formation, N₂O was introduced into the OFR to generate
272 NO_x resulting in 0–29 ppbv of NO concentrations. As shown in Figure 3, molar yields of formic
273 acid and acetic acid were not significantly affected by NO concentration under both 20% and
274 70% RH conditions. Even at the highest NO levels (~29 ppbv), which the ratio of NO
275 concentration to HO₂ radicals (simulated by model) exceeded 1000, substantial production
276 of organic acids (~40% for formic acid and ~20% for acetic acid at 20% RH) were also observed.



277 If organic acid formation were dominated by the peroxy radical pathway, such high NO: \cdot HO₂
278 ratios would be expected to strongly suppress their yields. However, at 70% RH, organic acid
279 yields even increased slightly with increasing NO concentrations. The observed lack of
280 suppression therefore provides strong evidence that a NO_x-insensitive pathway dominates
281 organic acid production during toluene photooxidation. This result is consistent with field
282 observations of rapid organic acid formation in polluted environments, where NO_x levels are
283 typically elevated (Veres et al., 2011; Yuan et al., 2015; Millet et al., 2015; Liggio et al., 2017),
284 and offers a plausible explanation for the persistent underestimation of organic acid
285 concentrations in atmospheric models under both pristine and polluted conditions (Stavrakou
286 et al., 2012; Yuan et al., 2015; Bannan et al., 2017; Khan et al., 2018).



287 **Figure 3.** NO_x dependence of formic acid and acetic acid yields under 20% RH (a) and 70%
288 RH (b) conditions. Error bars represent standard deviations from repeated experiments under
289 identical conditions.

290 **3.2 Underestimated Organic Acid Yields in Chemical Models**

291 To further assess the ability of current chemical mechanisms to reproduce observed organic
292 acid formation, we compared our experimental results with simulations using the MCM v3.3.1
293 model. For acetic acid, two formation pathways are included in MCM v3.3.1 (reactions R1 and
294 R2):

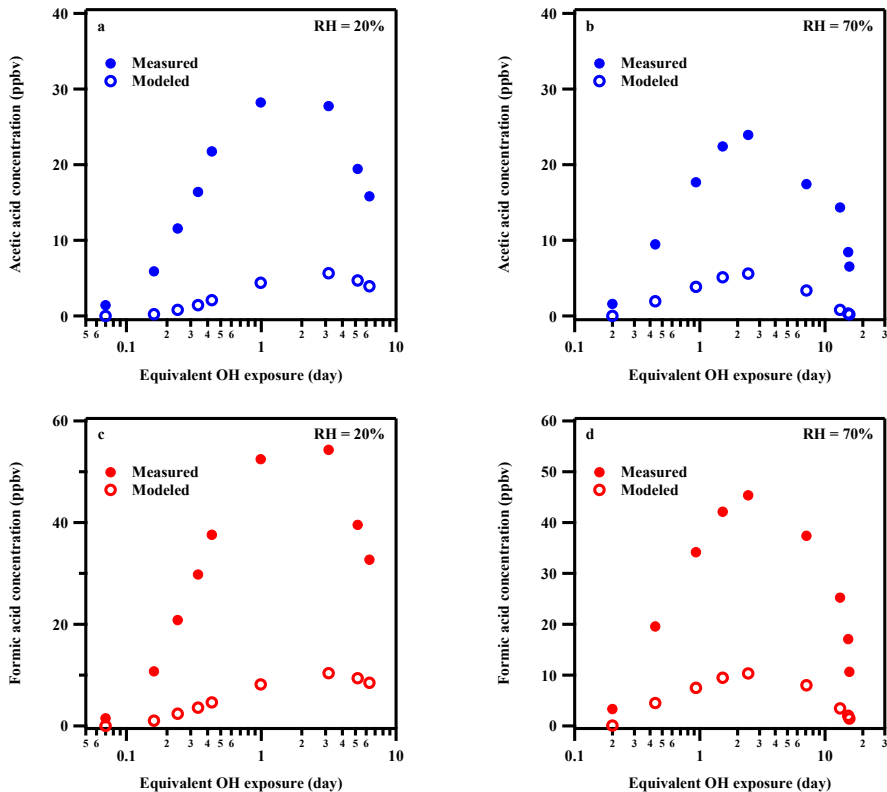


295 Model simulations indicate that reaction R2 ($\text{CH}_3\text{CO}_3\bullet + \text{RO}_2\bullet$) dominates acetic acid
296 production (>90%). While the model can reproduce the general trend of acetic acid
297 concentrations, initially increasing and then decreasing with $\cdot\text{OH}$ exposure, it substantially
298 underestimates the observed values. The maximum modeled yield (~7% at ~3 equivalent days)



299 is roughly five times lower than measured yields under both RH conditions (Figure 4a–b). This
300 discrepancy suggests that additional formation pathways, not included in the current model,
301 may significantly contribute to acetic acid production during toluene photooxidation.

302 It is noted that formic acid is not considered as the product of $\cdot\text{OH}$ oxidation of aromatic
303 compounds including toluene in the current model. Therefore, we implemented four candidate
304 pathways based on previous studies prior to model simulation (Yetter et al., 1989; Archibald et
305 al., 2007; Fittschen et al., 2014; Yuan et al., 2015; Shaw et al., 2018). (1). $\text{HOCH}_2\text{OO}\cdot$ chemistry:
306 Analogous to the acetic acid mechanism, formic acid can also be formed from either the reaction
307 of $\text{HOCH}_2\text{OO}\cdot$ with $\text{HO}_2\cdot$ or the bimolecular reaction of $\text{HOCH}_2\text{OO}\cdot$ (Jenkin et al., 2008; Yuan
308 et al., 2015). 2. Vinyl alcohol ($\text{CH}_2=\text{CHOH}$) oxidation: Formic acid formation via the OH
309 radical initiated oxidation of vinyl alcohol, which is generated through acetaldehyde
310 tautomerization. Both photo-induced and organic-acid-catalyzed tautomerization processes
311 were included (Archibald et al., 2007; Yuan et al., 2015; Shaw et al., 2018). 3. $\text{HCHO} + \cdot\text{OH}$
312 reaction: Direct formation through $\text{HCHO} + \cdot\text{OH} \rightarrow \text{HCOOH} + \text{H}$, with a rate coefficient of
313 $2.0 \times 10^{-13} \text{ cm}^3 \text{ molecule}^{-1} \text{ s}^{-1}$ (Yetter et al., 1989). 4. $\text{CH}_3\text{O}_2\cdot + \cdot\text{OH}$ reaction: Formic acid
314 formation via $\text{CH}_3\text{O}_2\cdot + \cdot\text{OH} \rightarrow \text{HCOOH} + \text{H}_2\text{O}$, with a very high rate coefficient of 2.8×10^{-10}
315 $\text{cm}^3 \text{ molecule}^{-1} \text{ s}^{-1}$ (Fittschen et al., 2014). Model evaluation indicates that pathways 1–3
316 contributed minimally (<1%). Pathway 1 ($\text{HOCH}_2\text{OO}\cdot$ chemistry) exhibits much lower yields
317 than the analogous acetic acid mechanism due to the low stability and consequently low
318 concentration of HOCH_2OO radicals relative to CH_3CO_3 radicals. Pathways 2 and 3 involve
319 aldehydes as precursors, which also limit formic acid production. Only pathway 4 ($\text{CH}_3\text{O}_2\cdot +$
320 $\cdot\text{OH}$) produced a substantial amount of formic acid, with a maximum modeled yield of ~13%
321 at ~3 equivalent days. However, the modeled concentrations of formic acid are still
322 approximately five times lower than the experimental measurements (Figure 4c–d). Pathway 4
323 is highly sensitive to NO_x , and our experimental results, which show that organic acid formation
324 is insensitive to NO_x levels, suggest that this pathway is unlikely to be the dominant mechanism
325 for organic acid production. Overall, these results indicate that the known pathways account for
326 only a small fraction of the observed formic and acetic acid production, implying the existence
327 of additional, yet unidentified, formation pathways for organic acids.



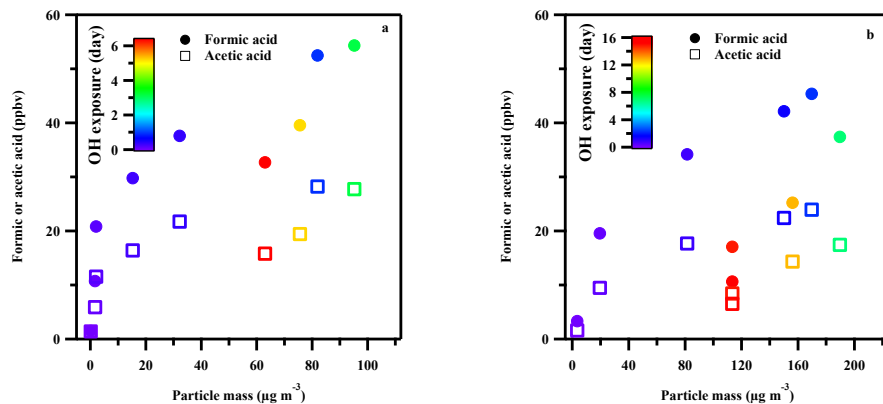
328 **Figure 4.** Comparison of measured and modeled concentrations of formic acid and acetic acid
329 at different OH exposures. (a) Acetic acid at 20% RH; (b) Acetic acid at 70% RH; (c) Formic
330 acid at 20% RH; (d) Formic acid at 70% RH.

331 **3.3 Organic Acids Formed from the Multi-generation oxidation**

332 Previous modeling studies have suggested that the aging of SOA could significantly contribute
333 to the atmospheric budgets of organic acids (Paulot et al., 2011), and laboratory experiments
334 have confirmed the production of organic acids during SOA photodegradation (Malecha and
335 Nizkorodov, 2016, 2017; Jiang et al., 2023). In this study, we analyzed the relationship between
336 SOA particle mass and organic acid production to evaluate this potential pathway. However,
337 the distinctly different temporal profiles of gas-phase organic acid production and SOA
338 formation (Figure 5) imply that SOA photodegradation is not the primary source of the observed
339 high organic acid yields. First, SOA formation exhibits a delay relative to the rapid production
340 of organic acids, consistent with the “incubation period” for aromatic SOA formation (Ng et al.,
341 2007; Wyche et al., 2009). Substantial organic acid yields are observed even mass concentration
342 of SOA is negligible (Figure 5a), effectively ruling out SOA photodegradation as the primary



343 source. Second, when gas-phase organic acid concentrations begin to decline, SOA mass
344 continues to increase (Figure 5), indicating decoupled formation and removal pathways for
345 SOA and organic acids. At very high $\cdot\text{OH}$ exposures (Figure 5b), while organic acid
346 concentrations decrease, SOA mass remains nearly unchanged. This suggests that gas-phase
347 organic acids are more reactive toward gas-phase oxidants than the more persistent SOA,
348 consistent with the generally longer lifetimes of aerosol-phase organics against oxidation
349 (Isaacman-VanWertz et al., 2018). Although SOA photodegradation can produce small
350 oxygenated VOCs (including formic and acetic acids), previous studies showed that aromatic-
351 derived SOA generates much lower yields of such products compared to biogenic SOA (e.g.,
352 from isoprene or α -pinene) (Malecha and Nizkorodov, 2016). These evidence support the
353 inference that SOA photodegradation may be not the main driver of the exceptionally high
354 formic and acetic acid yields observed during toluene photooxidation.

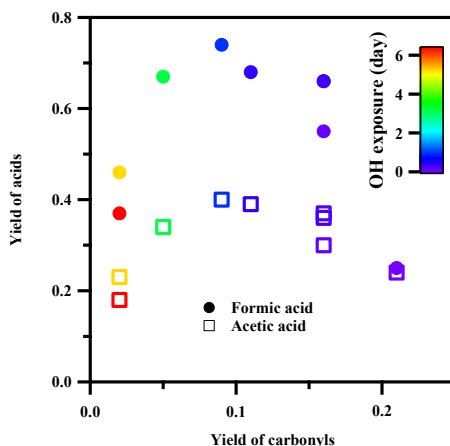


355 **Figure 5.** Correlations of particle mass concentration with gas-phase formic acid and acetic
356 acid during the photooxidation of toluene at different $\cdot\text{OH}$ exposure. a: 20% RH; b: 70% RH.
357 Color of marker represents different $\cdot\text{OH}$ exposure levels.

358 To further investigate the origin of the high organic acid yields observed during toluene
359 photooxidation, we first examined key first-generation ring-opened products, namely glyoxal
360 and methylglyoxal, which are well-known primary products in aromatic photooxidation
361 (Volkamer et al., 2001). In our experiments, the molar yields of these carbonyl compounds at
362 low $\cdot\text{OH}$ exposure are 11% and 10%, respectively, aligning with results reported in previous
363 studies (Gery et al., 1985; Bandow et al., 1985). Figure 6 displays that the yields of glyoxal and
364 methylglyoxal decreased rapidly with increasing $\cdot\text{OH}$ exposure, dropping to approximately 1%
365 at higher exposures. In contrast, the yields of formic and acetic acids showed a distinct
366 maximum at intermediate $\cdot\text{OH}$ exposures (1–3 equivalent days). Previous studies have



367 proposed that oxidation of glyoxal and methylglyoxal contributes to formic and acetic acid
368 formation (Paulot et al., 2011). But these pathways are excluded in this study given the
369 substantially lower yields of glyoxal and methylglyoxal observed. Moreover, the poor linear
370 correlation between the yields of formic acid and acetic acid and the first-generation ring-
371 opened products suggests that these acids are secondary or later-generation products formed
372 through multistep oxidation processes instead of the primary oxidation products. Previous study
373 elucidated that the fragmentation and further oxidation of five-membered oxygen-containing
374 heterocyclic compounds, which were important intermediates in the oxidation of aromatic
375 compounds, can yield acetic acid (Forstner et al., 1997; Bahreini et al., 2005; Walavalkar et al.,
376 2017). However, this pathway is still controversial due to the lack of robust evidence. The major
377 precursors and detailed mechanisms for the multigenerational oxidation resulting in the high
378 yield of formic acid and acetic acid during the photooxidation of toluene warrants further
379 investigations.



380
381 **Figure 6.** Correlations of yields of carbonyl compounds (sum of glyoxal and methylglyoxal)
382 with yields of gas-phase formic acid and acetic acid during the photooxidation of toluene at
383 different $\cdot\text{OH}$ exposure (20% RH). Markers are color-coded to represent different $\cdot\text{OH}$
384 exposure levels.

385 **4 ATMOSPHERIC IMPLICATIONS**

386 This study reveals unexpectedly high yields of formic acid (up to 74%) and acetic acid (up to
387 40%) during the multi-generational photooxidation of toluene, achieved over equivalent
388 atmospheric aging times of 1–3 days in our oxidation flow reactor experiments. The formation
389 of these organic acids showed minimal sensitivity to NO_x concentrations and relative humidity.
390 The up-to-date MCM v3.3.1 model substantially underestimates the observed organic acid



391 concentrations in the OFR. While both small gas-phase organic acids and low-volatility
392 particulate matter increase with atmospheric aging (within a certain degree of oxidation), their
393 differing production timescales suggest that photodegradation of SOA particles may not be the
394 dominant formation pathway for organic acids. Combined with the measurement of carbonyl
395 compounds, we proposed that the observed organic acids are predominantly from the multi-
396 generational oxidation of toluene. A mechanistic understanding of the multi-generation
397 oxidation of toluene, particularly the photooxidation of intermediate products such as maleic
398 anhydride, requires further exploration (Lu et al., 2024; Wang et al., 2024).

399 Our findings also provide new insight into understanding organic acid budgets in urban
400 atmospheres. Previous studies have observed rapid secondary production of organic acids in
401 urban air masses (Veres et al., 2011), but model simulations have significantly underestimated
402 their concentrations (Le Breton et al., 2012; Yuan et al., 2015). The high yields of formic and
403 acetic acids at elevated $\cdot\text{OH}$ exposures may help explain these discrepancies. Liggio et al. (2017)
404 found that the underestimation of organic acids increased with reaction time, while Yuan et al.
405 (2015) reported that the peak concentrations of formic acid occurred 4–6 days after the peak
406 benzene levels (Yuan et al., 2015; Liggio et al., 2017). In their studies, they evaluated the
407 contributions of aromatics to formic acid, assuming a yield of 15%, and concluded that
408 aromatics contribute about 11%–12% of the total formic acid production. If a yield of 74% is
409 adopted, the contributions of aromatics would be as high as 55%–60%. This outcome may
410 explain the remaining 50% of missing sources in the model after considering the known sources
411 (Yuan et al., 2015; Liggio et al., 2017). The large amounts of small gas-phase organic acids
412 produced from the photooxidation of aromatics in urban areas could further affect the aerosol
413 pH and the formation of particles. Additionally, while small organic acids such as formic and
414 acetic acid have long been recognized as useful tracers for atmospheric VOC oxidation and
415 SOA aging (Munger et al., 1986; Hansen et al., 2014), our results suggest that their utility as
416 reliable tracers for SOA production is limited to a relatively narrow $\cdot\text{OH}$ exposure window
417 (approximately 0.2–3 equivalent days). Beyond this range, their concentrations decouple from
418 SOA mass due to differences in reactivity and removal pathways (Isaacman-VanWertz et al.,
419 2018).

420

421 **Acknowledgements**

422 The authors gratefully thank the National Key Research and Development Program of China
423 (2022YFC3701102) for financial support.



424 **Author contributions**

425 ZC, LH, and HS designed the research. HS performed research, analyzed the data, and drafted
426 the initial manuscript. LH and ZC revised the manuscript. MZ and YY assisted with the model
427 simulation. YZ, HL, and HW provided valuable comments and suggestions for the manuscript.

428

429 **Competing interests**

430 All authors declare they have no competing interests.

431

432 **Data availability**

433 The data used in this study is available upon request from the corresponding author.

434

435 **References**

436 Archibald, A. T., McGillen, M. R., Taatjes, C. A., Percival, C. J., and Shallcross, D. E.:
437 Atmospheric transformation of enols: A potential secondary source of carboxylic acids in the
438 urban troposphere, *Geophys. Res. Lett.*, 34, 2007GL031032, 2007.

439 Bahreini, R., Keywood, M. D., Ng, N. L., Varutbangkul, V., Gao, S., Flagan, R. C., Seinfeld, J.
440 H., Worsnop, D. R., and Jimenez, J. L.: Measurements of Secondary Organic Aerosol from
441 Oxidation of Cycloalkenes, Terpenes, and *m*-Xylene Using an Aerodyne Aerosol Mass
442 Spectrometer, *Environ. Sci. Technol.*, 39, 5674–5688, 2005.

443 Baltensperger, U., Kalberer, M., Dommen, J., Paulsen, D., Alfarra, M. R., Coe, H., Fisseha, R.,
444 Gascho, A., Gysel, M., Nyeki, S., Sax, M., Steinbacher, M., Prevot, A. S. H., Sjögren, S.,
445 Weingartner, E., and Zenobi, R.: Secondary organic aerosols from anthropogenic and biogenic
446 precursors, *Faraday Discuss.*, 130, 265–278, 2005.

447 Bandow, H. and Washida, N.: Ring-cleavage Reactions of Aromatic Hydrocarbons Studied by
448 FT-IR Spectroscopy. III. Photooxidation of 1,2,3-, 1,2,4-, and 1,3,5-Trimethylbenzenes in the
449 NO_x-Air System, *Bull. Chem. Soc. Jpn.*, 58, 2549–2555, 1985.

450 Bandow, H., Washida, N., and Akimoto, H.: Ring-cleavage Reactions of Aromatic
451 Hydrocarbons Studied by FT-IR Spectroscopy. I. Photooxidation of Toluene and Benzene in
452 the NO_x-Air System, *Bull. Chem. Soc. Jpn.*, 58, 2531–2540, 1985.

453 Bannan, T. J., Murray Booth, A., Le Breton, M., Bacak, A., Muller, J. B. A., Leather, K. E.,
454 Khan, M. A. H., Lee, J. D., Dunmore, R. E., Hopkins, J. R., Fleming, Z. L., Sheps, L., Taatjes,
455 C. A., Shallcross, D. E., and Percival, C. J.: Seasonality of formic acid (HCOOH) in London
456 during the ClearLo campaign, *J. Geophys. Res. Atmospheres*, 122, 12,488-12,498, 2017.

457 Bates, K. H., Jacob, D. J., Cope, J. D., Chen, X., Millet, D. B., and Nguyen, T. B.: Emerging



458 investigator series: aqueous oxidation of isoprene-derived organic aerosol species as a source
459 of atmospheric formic and acetic acids, *Environ. Sci. Atmospheres*, 3, 1651–1664, 2023.

460 Battin-Leclerc, F., Konnov, A. A., Jaffrezo, J. L., and Legrand, M.: To Better Understand the
461 Formation of Short-Chain Acids in Combustion Systems, *Combust. Sci. Technol.*, 180, 343–
462 370, 2007.

463 Berndt, T. and Böge, O.: Gas-phase reaction of OH radicals with benzene: products and
464 mechanism, *Phys. Chem. Chem. Phys.*, 3, 4946–4956, 2001.

465 Berndt, T., Böge, O., and Herrmann, H.: On the formation of benzene oxide/oxepin in the gas-
466 phase reaction of OH radicals with benzene, *Chem. Phys. Lett.*, 314, 435–442, 1999.

467 Brune, W. H.: The Chamber Wall Index for Gas–Wall Interactions in Atmospheric
468 Environmental Enclosures, *Environ. Sci. Technol.*, 53, 3645–3652, 2019.

469 Bruns, E. A., El Haddad, I., Keller, A., Klein, F., Kumar, N. K., Pieber, S. M., Corbin, J. C.,
470 Slowik, J. G., Brune, W. H., Baltensperger, U., and Prévôt, A. S. H.: Inter-comparison of
471 laboratory smog chamber and flow reactor systems on organic aerosol yield and composition,
472 *Atmospheric Meas. Tech.*, 8, 2315–2332, 2015.

473 Bruns, E. A., Slowik, J. G., El Haddad, I., Kılıç, D., Klein, F., Dommen, J., Temime-Roussel,
474 B., Marchand, N., Baltensperger, U., and Prévôt, A. S. H.: Characterization of gas-phase
475 organics using proton transfer reaction time-of-flight mass spectrometry: fresh and aged
476 residential wood combustion emissions, *Atmospheric Chem. Phys.*, 17, 705–720, 2017.

477 Chaliyakunnel, S., Millet, D. B., Wells, K. C., Cady-Pereira, K. E., and Shephard, M. W.: A
478 Large Underestimate of Formic Acid from Tropical Fires: Constraints from Space-Borne
479 Measurements, *Environ. Sci. Technol.*, 50, 5631–5640, 2016.

480 Chebbi, A. and Carlier, P.: Carboxylic acids in the troposphere, occurrence, sources, and sinks:
481 A review, *Atmos. Environ.*, 30, 4233–4249, 1996.

482 Ding, Z., Zhu, Y., Wang, G., Li, H., Xu, J., Tian, M., Liu, Z., Chen, J., Yun, L., Zheng, H., Gui,
483 H., Liu, J., Li, R., Deng, C., and Huang, K.: Coastal eutrophic ecosystem as an overlooked pool
484 of atmospheric formic acid: disentangling biogenic and abiotic contributions, *Environ. Sci.*
485 *Technol. Lett.*, 2025.

486 Drozd, G. T., Zhao, Y., Saliba, G., Frodin, B., Maddox, C., Oliver Chang, M.-C., Maldonado,
487 H., Sardar, S., Weber, R. J., Robinson, A. L., and Goldstein, A. H.: Detailed Speciation of
488 Intermediate Volatility and Semivolatile Organic Compound Emissions from Gasoline Vehicles:
489 Effects of Cold-Starts and Implications for Secondary Organic Aerosol Formation, *Environ. Sci.*
490 *Technol.*, 53, 1706–1714, 2019.

491 Fittschen, C., Whalley, L. K., and Heard, D. E.: The reaction of CH_3O_2 radicals with OH radicals:



492 a neglected sink for CH_3O_2 in the remote atmosphere, *Environ. Sci. Technol.*, 48, 7700–7701,
493 2014.

494 Forstner, H. J. L., Flagan, R. C., and Seinfeld, J. H.: Secondary Organic Aerosol from the
495 Photooxidation of Aromatic Hydrocarbons: Molecular Composition, *Environ. Sci. Technol.*, 31,
496 1345–1358, 1997.

497 Franco, B., Blumenstock, T., Cho, C., Clarisse, L., Clerbaux, C., Coheur, P.-F., De Mazière, M.,
498 De Smedt, I., Dorn, H.-P., Emmerichs, T., Fuchs, H., Gkatzelis, G., Griffith, D. W. T., Gromov,
499 S., Hannigan, J. W., Hase, F., Hohaus, T., Jones, N., Kerkweg, A., Kiendler-Scharr, A., Lutsch,
500 E., Mahieu, E., Novelli, A., Ortega, I., Paton-Walsh, C., Pommier, M., Pozzer, A., Reimer, D.,
501 Rosanka, S., Sander, R., Schneider, M., Strong, K., Tillmann, R., Van Roozendael, M.,
502 Vereecken, L., Vigouroux, C., Wahner, A., and Taraborrelli, D.: Ubiquitous atmospheric
503 production of organic acids mediated by cloud droplets, *Nature*, 593, 233–237, 2021.

504 Friedman, B. and Farmer, D. K.: SOA and gas phase organic acid yields from the sequential
505 photooxidation of seven monoterpenes, *Atmos. Environ.*, 187, 335–345, 2018.

506 Friedman, B., Link, M. F., Fulgham, S. R., Brophy, P., Galang, A., Brune, W. H., Jathar, S. H.,
507 and Farmer, D. K.: Primary and Secondary Sources of Gas-Phase Organic Acids from Diesel
508 Exhaust, *Environ. Sci. Technol.*, 51, 10872–10880, 2017.

509 Gery, M. W., Fox, D. L., Jeffries, H. E., Stockburger, L., and Weathers, W. S.: A continuous
510 stirred tank reactor investigation of the gas-phase reaction of hydroxyl radicals and toluene, *Int.*
511 *J. Chem. Kinet.*, 17, 931–955, 1985.

512 Hansen, A. M. K., Kristensen, K., Nguyen, Q. T., Zare, A., Cozzi, F., Nøjgaard, J. K., Skov, H.,
513 Brandt, J., Christensen, J. H., Ström, J., Tunved, P., Krejci, R., and Glasius, M.: Organosulfates
514 and organic acids in Arctic aerosols: speciation, annual variation and concentration levels,
515 *Atmospheric Chem. Phys.*, 14, 7807–7823, 2014.

516 Huang, D., Chen, Z. M., Zhao, Y., and Liang, H.: Newly observed peroxides and the water
517 effect on the formation and removal of hydroxyalkyl hydroperoxides in the ozonolysis of
518 isoprene, *Atmospheric Chem. Phys.*, 13, 5671–5683, 2013.

519 Isaacman-VanWertz, G., Massoli, P., O'Brien, R., Lim, C., Franklin, J. P., Moss, J. A., Hunter,
520 J. F., Nowak, J. B., Canagaratna, M. R., Misztal, P. K., Arata, C., Roscioli, J. R., Herndon, S.
521 T., Onasch, T. B., Lambe, A. T., Jayne, J. T., Su, L., Knopf, D. A., Goldstein, A. H., Worsnop,
522 D. R., and Kroll, J. H.: Chemical evolution of atmospheric organic carbon over multiple
523 generations of oxidation, *Nat. Chem.*, 10, 462–468, 2018.

524 Jenkin, M. E., Hurley, M. D., and Wallington, T. J.: Investigation of the radical product channel
525 of the $\text{CH}_3\text{C}(\text{O})\text{CH}_2\text{O}_2 + \text{HO}_2$ reaction in the gas phase, *Phys. Chem. Chem. Phys.*, 10, 4274–
526 4280, 2008.



527 Jenkin, M. E., Young, J. C., and Rickard, A. R.: The MCM v3.3.1 degradation scheme for
528 isoprene, *Atmospheric Chem. Phys.*, 15, 11433–11459, 2015.

529 Jiang, Y., Xia, M., Wang, Z., Zheng, P., Chen, Y., and Wang, T.: Photochemical ageing of
530 aerosols contributes significantly to the production of atmospheric formic acid, *Atmospheric*
531 *Chem. Phys.*, 23, 14813–14828, 2023.

532 Kang, M., Zhang, H., and Ying, Q.: Sulfate or organic acids: the atmospheric fate of stabilized
533 criegee intermediates, *J. Geophys. Res. Atmospheres*, 130, e2025JD044867, 2025.

534 Keller-Rudek, H., Moortgat, G. K., Sander, R., and Sørensen, R.: The MPI-Mainz UV/VIS
535 Spectral Atlas of Gaseous Molecules of Atmospheric Interest, *Earth Syst. Sci. Data*, 5, 365–373,
536 2013.

537 Khan, M. A. H., Lyons, K., Chhantyal-Pun, R., McGillen, M. R., Caravan, R. L., Taatjes, C. A.,
538 Orr-Ewing, A. J., Percival, C. J., and Shallcross, D. E.: Investigating the tropospheric chemistry
539 of acetic acid using the global 3-D chemistry transport model, STOCHEM-CRI, *J. Geophys.*
540 *Res. Atmospheres*, 123, 6267–6281, 2018.

541 Lambe, A., Massoli, P., Zhang, X., Canagaratna, M., Nowak, J., Daube, C., Yan, C., Nie, W.,
542 Onasch, T., Jayne, J., Kolb, C., Davidovits, P., Worsnop, D., and Brune, W.: Controlled nitric
543 oxide production via $O(^1D) + N_2O$ reactions for use in oxidation flow reactor studies,
544 *Atmospheric Meas. Tech.*, 10, 2283–2298, 2017.

545 Lambe, A. T., Onasch, T. B., Croasdale, D. R., Wright, J. P., Martin, A. T., Franklin, J. P.,
546 Massoli, P., Kroll, J. H., Canagaratna, M. R., Brune, W. H., Worsnop, D. R., and Davidovits, P.:
547 Transitions from Functionalization to Fragmentation Reactions of Laboratory Secondary
548 Organic Aerosol (SOA) Generated from the OH Oxidation of Alkane Precursors, *Environ. Sci.*
549 *Technol.*, 46, 5430–5437, 2012.

550 Lambe, A. T., Cappa, C. D., Massoli, P., Onasch, T. B., Forestieri, S. D., Martin, A. T.,
551 Cummings, M. J., Croasdale, D. R., Brune, W. H., Worsnop, D. R., and Davidovits, P.: Relationship
552 between Oxidation Level and Optical Properties of Secondary Organic Aerosol,
553 *Environ. Sci. Technol.*, 47, 6349–6357, 2013.

554 Lambe, A. T., Chhabra, P. S., Onasch, T. B., Brune, W. H., Hunter, J. F., Kroll, J. H., Cummings,
555 M. J., Brogan, J. F., Parmar, Y., Worsnop, D. R., Kolb, C. E., and Davidovits, P.: Effect of
556 oxidant concentration, exposure time, and seed particles on secondary organic aerosol chemical
557 composition and yield, *Atmospheric Chem. Phys.*, 15, 3063–3075, 2015.

558 Le Breton, M., McGillen, M. R., Muller, J. B. A., Bacak, A., Shallcross, D. E., Xiao, P., Huey,
559 L. G., Tanner, D., Coe, H., and Percival, C. J.: Airborne observations of formic acid using a
560 chemical ionization mass spectrometer, *Atmospheric Meas. Tech.*, 5, 3029–3039, 2012.

561 Li, R., Palm, B. B., Ortega, A. M., Hlywiak, J., Hu, W., Peng, Z., Day, D. A., Knote, C., Brune,



562 W. H., De Gouw, J. A., and Jimenez, J. L.: Modeling the Radical Chemistry in an Oxidation
563 Flow Reactor: Radical Formation and Recycling, Sensitivities, and the OH Exposure
564 Estimation Equation, *J. Phys. Chem. A*, 119, 4418–4432, 2015.

565 Liggio, J., Moussa, S. G., Wentzell, J., Darlington, A., Liu, P., Leithead, A., Hayden, K.,
566 O'Brien, J., Mittermeier, R. L., Staebler, R., Wolde, M., and Li, S.-M.: Understanding the
567 primary emissions and secondary formation of gaseous organic acids in the oil sands region of
568 Alberta, *Atmospheric Chem. Phys.*, 17, 8411–8427, 2017.

569 Link, M. F., Nguyen, T. B., Bates, K., Müller, J.-F., and Farmer, D. K.: Can Isoprene Oxidation
570 Explain High Concentrations of Atmospheric Formic and Acetic Acid over Forests?, *ACS Earth*
571 *Space Chem.*, 4, 730–740, 2020.

572 Lu, R., Zhou, P., Ma, F., Zhao, Q., Peng, X., Chen, J., and Xie, H.-B.: Multi-generation
573 oxidation mechanism of *M*-xylene: unexpected implications for secondary organic aerosol
574 formation, *Atmos. Environ.*, 327, 120511, 2024.

575 Malecha, K. T. and Nizkorodov, S. A.: Photodegradation of Secondary Organic Aerosol
576 Particles as a Source of Small, Oxygenated Volatile Organic Compounds, *Environ. Sci.*
577 *Technol.*, 50, 9990–9997, 2016.

578 Malecha, K. T. and Nizkorodov, S. A.: Feasibility of photosensitized reactions with secondary
579 organic aerosol particles in the presence of volatile organic compounds, *J. Phys. Chem. A*, 121,
580 4961–4967, 2017.

581 Millet, D. B., Baasandorj, M., Farmer, D. K., Thornton, J. A., Baumann, K., Brophy, P.,
582 Chaliyakunnel, S., De Gouw, J. A., Graus, M., Hu, L., Koss, A., Lee, B. H., Lopez-Hilfiker, F.,
583 Neuman, J. A., Paulot, F., Peischl, J., Pollack, I. B., Ryerson, T. B., Warneke, C., Williams,
584 B. J., and Xu, J.: A large and ubiquitous source of atmospheric formic acid, *Atmospheric Chem.*
585 *Phys.*, 15, 6283–6304, 2015.

586 Müller, M., Graus, M., Wisthaler, A., Hansel, A., Metzger, A., Dommen, J., and Baltensperger,
587 U.: Analysis of high mass resolution PTR-TOF mass spectra from 1,3,5-trimethylbenzene
588 (TMB) environmental chamber experiments, *Atmospheric Chem. Phys.*, 12, 829–843, 2012.

589 Mungall, E. L., Abbatt, J. P. D., Wentzell, J. J. B., Wentworth, G. R., Murphy, J. G., Kunkel, D.,
590 Gute, E., Tarasick, D. W., Sharma, S., Cox, C. J., Uttal, T., and Liggio, J.: High gas-phase
591 mixing ratios of formic and acetic acid in the High Arctic, *Atmospheric Chem. Phys.*, 18,
592 10237–10254, 2018.

593 Munger, J. W., Tiller, C., and Hoffmann, M. R.: Identification of hydroxymethanesulfonate in
594 fog water, *Science*, 231, 247–249, 1986.

595 Murschell, T. and Farmer, D. K.: Atmospheric OH oxidation of three chlorinated aromatic
596 herbicides, *Environ. Sci. Technol.*, 52, 4583–4591, 2018.



597 Neeb, P., Sauer, F., Horie, O., and Moortgat, G. K.: Formation of hydroxymethyl hydroperoxide
598 and formic acid in alkene ozonolysis in the presence of water vapour, *Atmos. Environ.*, 31,
599 1417–1423, 1997.

600 Ng, N. L., Kroll, J. H., Chan, A. W. H., Chhabra, P. S., Flagan, R. C., and Seinfeld, J. H.:
601 Secondary organic aerosol formation from m-xylene, toluene, and benzene, *Atmospheric Chem.
602 Phys.*, 7, 3909–3922, 2007.

603 Ortega, A. M., Day, D. A., Cubison, M. J., Brune, W. H., Bon, D., De Gouw, J. A., and Jimenez,
604 J. L.: Secondary organic aerosol formation and primary organic aerosol oxidation from
605 biomass-burning smoke in a flow reactor during FLAME-3, *Atmospheric Chem. Phys.*, 13,
606 11551–11571, 2013.

607 Orzechowska, G. E. and Paulson, S. E.: Photochemical sources of organic acids. 1. Reaction of
608 ozone with isoprene, propene, and 2-butenes under dry and humid conditions using SPME, *J.
609 Phys. Chem. A*, 109, 5358–5365, 2005.

610 Paulot, F., Wunch, D., Crounse, J. D., Toon, G. C., Millet, D. B., DeCarlo, P. F., Vigouroux, C.,
611 Deutscher, N. M., González Abad, G., Notholt, J., Warneke, T., Hannigan, J. W., Warneke, C.,
612 De Gouw, J. A., Dunlea, E. J., De Mazière, M., Griffith, D. W. T., Bernath, P., Jimenez, J. L.,
613 and Wennberg, P. O.: Importance of secondary sources in the atmospheric budgets of formic
614 and acetic acids, *Atmospheric Chem. Phys.*, 11, 1989–2013, 2011.

615 Peng, Z., Day, D. A., Stark, H., Li, R., Lee-Taylor, J., Palm, B. B., Brune, W. H., and Jimenez,
616 J. L.: HO_x radical chemistry in oxidation flow reactors with low-pressure mercury lamps
617 systematically examined by modeling, *Atmospheric Meas. Tech.*, 8, 4863–4890, 2015.

618 Peng, Z., Day, D. A., Ortega, A. M., Palm, B. B., Hu, W., Stark, H., Li, R., Tsigaridis, K., Brune,
619 W. H., and Jimenez, J. L.: Non-OH chemistry in oxidation flow reactors for the study of
620 atmospheric chemistry systematically examined by modeling, *Atmospheric Chem. Phys.*, 16,
621 4283–4305, 2016.

622 Praplan, A. P., Hegyi-Gaeggeler, K., Barmet, P., Pfaffenberger, L., Dommen, J., and
623 Baltensperger, U.: Online measurements of water-soluble organic acids in the gas and aerosol
624 phase from the photooxidation of 1,3,5-trimethylbenzene, *Atmospheric Chem. Phys.*, 14, 8665–
625 8677, 2014.

626 Schobesberger, S., Lopez-Hilfiker, F. D., Taipale, D., Millet, D. B., D'Ambro, E. L., Rantala,
627 P., Mammarella, I., Zhou, P., Wolfe, G. M., Lee, B. H., Boy, M., and Thornton, J. A.: High
628 upward fluxes of formic acid from a boreal forest canopy, *Geophys. Res. Lett.*, 43, 9342–9351,
629 2016.

630 Seuwen, R. and Warneck, P.: Oxidation of toluene in NO_x free air: product distribution and
631 mechanism, *Int. J. Chem. Kinet.*, 28, 315–332, 1996.



632 Shaw, M. F., Sztáray, B., Whalley, L. K., Heard, D. E., Millet, D. B., Jordan, M. J. T., Osborn,
633 D. L., and Kable, S. H.: Photo-tautomerization of acetaldehyde as a photochemical source of
634 formic acid in the troposphere, *Nat. Commun.*, 9, 2584, 2018.

635 Shen, H., Chen, Z., Li, H., Qian, X., Qin, X., and Shi, W.: Gas-particle partitioning of carbonyl
636 compounds in the ambient atmosphere, *Environ. Sci. Technol.*, 52, 10997–11006, 2018.

637 Shen, H., Huang, L., Qian, X., Qin, X., and Chen, Z.: Positive Feedback between Partitioning
638 of Carbonyl Compounds and Particulate Sulfur Formation during Haze Episodes, *Environ. Sci.*
639 *Technol.*, 58, 21286–21294, 2024.

640 Stavrakou, T., Müller, J.-F., Peeters, J., Razavi, A., Clarisse, L., Clerbaux, C., Coheur, P.-F.,
641 Hurtmans, D., De Mazière, M., Vigouroux, C., Deutscher, N. M., Griffith, D. W. T., Jones, N.,
642 and Paton-Walsh, C.: Satellite evidence for a large source of formic acid from boreal and
643 tropical forests, *Nat. Geosci.*, 5, 26–30, 2012.

644 Tan, Z., Rohrer, F., Lu, K., Ma, X., Bohn, B., Broch, S., Dong, H., Fuchs, H., Gkatzelis, G. I.,
645 Hofzumahaus, A., Holland, F., Li, X., Liu, Y., Liu, Y., Novelli, A., Shao, M., Wang, H., Wu, Y.,
646 Zeng, L., Hu, M., Kiendler-Scharr, A., Wahner, A., and Zhang, Y.: Wintertime photochemistry
647 in Beijing: observations of RO_x radical concentrations in the North China Plain during the
648 BEST-ONE campaign, *Atmospheric Chem. Phys.*, 18, 12391–12411, 2018.

649 Tao, Y. and Murphy, J. G.: Evidence for the Importance of Semivolatile Organic Ammonium
650 Salts in Ambient Particulate Matter, *Environ. Sci. Technol.*, 53, 108–116, 2019.

651 Veres, P. R., Roberts, J. M., Cochran, A. K., Gilman, J. B., Kuster, W. C., Holloway, J. S., Graus,
652 M., Flynn, J., Lefer, B., Warneke, C., and de Gouw, J.: Evidence of rapid production of organic
653 acids in an urban air mass, *Geophys. Res. Lett.*, 38, 2011.

654 Volkamer, R., Platt, U., and Wirtz, K.: Primary and Secondary Glyoxal Formation from
655 Aromatics: Experimental Evidence for the Bicycloalkyl–Radical Pathway from Benzene,
656 Toluene, and *p*-Xylene, *J. Phys. Chem. A*, 105, 7865–7874, 2001.

657 Walavalkar, M. P., Sharma, A., Dhanya, S., and Naik, P. D.: Reactions of lactones with
658 tropospheric oxidants: A kinetics and products study, *Atmos. Environ.*, 161, 18–26, 2017.

659 Wang, Y., Li, C., Zhang, Y., Li, Y., Yang, G., Yang, X., Wu, Y., Yao, L., Zhang, H., and Wang,
660 L.: Secondary reactions of aromatics-derived oxygenated organic molecules lead to plentiful
661 highly oxygenated organic molecules within an intraday OH exposure, *Atmospheric Chem.*
662 *Phys.*, 24, 7961–7981, 2024.

663 Wu, H., Wang, Y., Li, H., Huang, L., Huang, D., Shen, H., Xing, Y., and Chen, Z.: The OH-
664 initiated oxidation of atmospheric peroxyacetic acid: Experimental and model studies, *Atmos.*
665 *Environ.*, 164, 61–70, 2017.



666 Wyche, K. P., Monks, P. S., Ellis, A. M., Cordell, R. L., Parker, A. E., Whyte, C., Metzger, A.,
667 Dommen, J., Duplissy, J., Prevot, A. S. H., Baltensperger, U., Rickard, A. R., and Wulfert, F.:
668 Gas phase precursors to anthropogenic secondary organic aerosol: detailed observations of
669 1,3,5-trimethylbenzene photooxidation, *Atmospheric Chem. Phys.*, 9, 635–665, 2009.

670 Xing, Y., Li, H., Huang, L., Wu, H., Shen, H., and Chen, Z.: The production of formaldehyde
671 and hydroxyacetone in methacrolein photooxidation: New insights into mechanism and effects
672 of water vapor, *J. Environ. Sci.*, 66, 1–11, 2018.

673 Yetter, R. A., Rabitz, H., Dryer, F. L., Maki, R. G., and Klemm, R. B.: Evaluation of the rate
674 constant for the reaction OH+H₂CO: Application of modeling and sensitivity analysis
675 techniques for determination of the product branching ratio, *J. Chem. Phys.*, 91, 4088–4097,
676 1989.

677 Yuan, B., Veres, P. R., Warneke, C., Roberts, J. M., Gilman, J. B., Koss, A., Edwards, P. M.,
678 Graus, M., Kuster, W. C., Li, S.-M., Wild, R. J., Brown, S. S., Dubé, W. P., Lerner, B. M.,
679 Williams, E. J., Johnson, J. E., Quinn, P. K., Bates, T. S., Lefer, B., Hayes, P. L., Jimenez, J. L.,
680 Weber, R. J., Zamora, R., Ervens, B., Millet, D. B., Rappenglück, B., and De Gouw, J. A.:
681 Investigation of secondary formation of formic acid: urban environment vs. oil and gas
682 producing region, *Atmospheric Chem. Phys.*, 15, 1975–1993, 2015.

683 Zervas, E.: Formation of organic acids from propane, isoctane and toluene/isoctane flames,
684 *Fuel*, 84, 691–700, 2005.

685 Zhang, X., Cappa, C. D., Jathar, S. H., McVay, R. C., Ensberg, J. J., Kleeman, M. J., and
686 Seinfeld, J. H.: Influence of vapor wall loss in laboratory chambers on yields of secondary
687 organic aerosol, *Proc. Natl. Acad. Sci.*, 111, 5802–5807, 2014.

688